Journal of Heat and Mass Transfer Research

Journal homepage: http://jhmtr.journals.semnan.ac.ir

Semnan University

Using Burnett Equations to Derive an Analytical Solution to Pressure-Driven Gas Flow and Heat Transfer in Micro-Couette Flow

Ahmad Reza Rahmati*, Faezeh Nejati Barzoki

Department of Mechanical Engineering, University of Khashan, Kashan, Iran

PAPER INFO

Paper history:
Received: 2016-12-29
Received: 2017-10-05
Accepted: 2017-10-12

Keywords:
Burnett equations;
Knudsen number;
Micro-Couette;
Pressure gradient;
Thermal flow;
Transition regime.

ABSTRACT

The aim of the present study is deriving an analytical solution to incompressible thermal flow in a micro-Couette geometry in the presence of a pressure gradient using Burnett equations with first- and second-order slip boundary conditions. The lower plate of the micro-Couette structure is stationary, whereas the upper plate moves at a constant velocity. Non-dimensional axial velocity and temperature profiles were obtained using the slip boundary conditions and were compared with the transition flow regime ($0.1 \leqslant Kn \leqslant 10$). The results showed that in this regime, rarefaction exerts a considerable effect on both the velocity and the temperature profiles. Because of the presence of the pressure gradient in the direction of the flow, the non-dimensional velocity and temperature profiles behave in a parabolic trend and flatten as the Knudsen number increases. The Poiseuille and Nusselt numbers, obtained using the derived analytical solution, decrease with increasing the Knudsen number. In the absence of an axial pressure gradient, the velocity profile behaves linearly and shows good agreement with the results of the previous works.

DOI: 10.22075/jhmtr.2017.1775.1131

1. Introduction

In recent years, the study of gas flow and heat transfer in micro-scale devices has become more prevalent in many scientific fields, e.g., microelectromechanical systems and the potential applications of micro-devices in engineering, medical sciences. Such interest is largely driven by the need for new technical tools which accurately predict the micro-scale transport processes and devices that are characterized by performance-enhancing designs [1]. Recent advances in micro/nanotechnology have enabled the manufacture of mechanical devices such as micro-channels, nozzles, and pumps. With these devices, porous media can be employed for micro-filtration, fractionation, catalysis, and microbiology-related applications. Micro-devices have also benefitted from the use of charged porous media structures, which are intended to magnify pumping, mixing, and separation effects [2].

Explorations into gas flow and its heat transfer characteristics in micro-geometries typically take the form of numerical and experimental research (e.g., [3–5]). In such studies, micro-Couette flow is regarded as an important problem in fluid mechanics since it is widely implicated in hydrodynamic lubrication, polymer/food processing, and viscometry, among other processes [6]. It also provides insight into the generation of unsteady boundary layers. A Couette flow-based approach is a suitable modeling method for micro-flows and a simple analogue for applications such as hard-disc drive reader heads, micro-turbines, and gas bearings. For the purpose of examining Couette

* Corresponding Author: A. R. Rahmati, Department of Mechanical Engineering, University of Kashan, Kashan, Iran.
Email: ar_rahmati@kashanu.ac.ir

flow, researchers perform a Chapman–Enskog expansion of the Boltzmann equation with the Knudsen number as a parameter, subsequently producing zero-order Euler equations, first-order Navier–Stokes equations, and second-order Burnett equations [7, 8]. Xue et al. [9], for instance, analyzed micro-Couette flow and heat transfer using Burnett equations. The authors found that rarefaction exerts a significant effect on the distribution of velocity, temperature, and pressure when flow enters the transition regime in isothermal walls or when the temperature ratio is high in non-isothermal walls.

Walls and Abedian [10] investigated the bivelocity gas dynamics of micro-channel Coquette flow to elucidate the characteristics of monoatomic Maxwellian gas flow in the micro-channel. Their results indicated that numerical predictions of density, temperature, and velocity distributions differ from those obtained using Burnett equations. Singh et al. [11] analytically solved the Burnett equations for plane Poiseuille flow and obtained a normalized mass flow rate, friction factor, and axial velocity profile which reveals a very good agreement with their experimental and simulation data. The analytical solution derived by the authors also predicts changes in the curvature of a streamwise pressure profile. Singh et al. [12] analyzed a solution of plane Couette flow in the transition regime and compared it with direct simulation Monte Carlo (DSMC) data. Good agreement between the results was observed up to a Knudsen number (*Kn*) equal to 10. Their results also enabled the formulation of a slip relationship, which can potentially provide a more accurate slip velocity in the transition regime than those from Maxwell's slip model. Lockerby and Reese [13] conducted high-resolution Burnett simulations of micro-Couette flow and heat transfer. The results on high-resolution numerical grids showed good agreement with data obtained from direct simulation methods. Xue et al. [14] analyzed the gaseous micro-Couette flow utilizing the DSMC method, Navier–Stokes equations, and Burnette equations. Finally, they compared the results of the three approaches.

Several researchers have also investigated the effects of pressure-driven flow in micro-channels. Zahid et al. [15], for instance, examined the Couette–Poiseuille flow of a gas in long micro-channels. In their work, the gas was shear driven and subjected to a pressure gradient. They comprehensively studied the effects of rarefaction and compressibility on flow characteristics and found the parallel flow assumption to be invalid in cases characterized by slight rarefaction. Finally, the authors found that axial and vertical velocity components depend on the degree of rarefaction, utilized pressure gradient, and wall velocity. Beskok et al. [16] carried out a detailed examination of the effects of rarefaction and compressibility on pressure-driven and shear-driven micro-flows. The authors discovered that rarefaction and compressibility phenomena need to be considered in micro-fluidic investigation. Jang and Wereley [17] studied the pressure distribution of gaseous flow in rectangular micro-channels and revealed that the deviation of pressure distributions from linear distribution decreases with augmentation of rarefaction. Bao and Lin [18] performed a Burnett simulation of compressible gas flow and heat transfer in micro-Poiseuille flow in the slip and transition flow regimes. It was concluded that with enhancement of Knudsen number, the Poiseuill number decreases and the Nusselt number would increase.

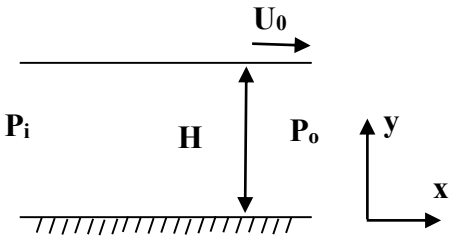

Figure 1. Couette flow coordinate system.

The present study extends the mentioned earlier works by using Burnett equations in order to capture an analytical solution to micro-Couette flow in the presence of a pressure gradient. The research concentrated on the flow and heat transfer behaviors of the Couette flow and compared these with first- and second-order boundary conditions. The results manifested that in the presence of a pressure gradient, the velocity profile converts from a linear profile into a parabolic one. Furthermore, an increase in the Knudsen number elevates the slip on the wall of the examined geometry and smoothens the temperature and velocity profiles.

2. Burnett equations applied to micro-Couette flow

In the present work, gas flow between two parallel infinite flat plates was considered the Couette flow (Fig. 1). The space between the plates is separated by a distance H. The lower plate is stationary, whereas the upper plate moves at a constant velocity U0. The gas flow is driven by the pressure difference between inlet pressure pi and outlet pressure po. The Burnett

equations were simplified under the assumption that the flow is steady, two-dimensional, fully developed, and incompressible. A pressure gradient was applied in the axial direction.

The general tensor expression of Burnett-level stress tensor [19] is presented in Eq. (1).

$$\sigma_{ij} = -2\mu\frac{\overline{\partial u_i}}{\partial x_j} + \frac{\mu^2}{p}\left[\omega_1\frac{\partial u_k}{\partial x_k}\frac{\overline{\partial u_i}}{\partial x_j} + \omega_2\left(\frac{D}{Dt}\frac{\overline{\partial u_i}}{\partial x_j} - 2\frac{\partial u_i}{\partial x_k}\frac{\partial u_k}{\partial x_j}\right) + \omega_3 R\frac{\partial^2 T}{\partial x_i \partial x_j}\right] + \frac{\mu^2}{p}\left[\omega_4\frac{1}{\rho T}\frac{\partial p}{\partial x_i}\frac{\partial T}{\partial x_j} + \omega_5\frac{R}{T}\frac{\partial T}{\partial x_i}\frac{\partial T}{\partial x_j} + \omega_6\frac{\partial u_i}{\partial x_k}\frac{\partial u_k}{\partial x_j}\right] \quad (1)$$

Where coefficients ω_i depend on the gas model. The Couette length (L) is considered to be much greater than the Couette height (H). Thus, $\varepsilon \equiv H/L \ll 1$

Burnett equations can be extensively simplified, thus generating terms that include $O(\epsilon)$ up to $O(\epsilon^5)$. The results of this expansion, including those on $O(\epsilon)$ terms, are presented in [19]. With $O(\varepsilon)$ terms disregarded, x and y momentum equations can be substantially simplified as follows:

$$\frac{\partial p}{\partial x}\left[1 - (\omega_2/3 + \omega_6/12)\frac{\mu^2}{p^2}\left(\frac{\partial u}{\partial y}\right)^2\right] = \mu\frac{\partial^2 u}{\partial y^2} + O(\epsilon) \quad (2)$$

$$\frac{\partial p}{\partial y} + (\omega_6/12 - 2\,\omega_2/3)\frac{\partial}{\partial y}\left[\frac{\mu^2}{p}\left(\frac{\partial u}{\partial y}\right)^2\right] = O(\epsilon) \quad (3)$$

Under the assumption of a Maxwellian gas model, for which coefficients $(\omega_1, \omega_2, \omega_6)$ = (10/3, 2, 8) [20], and non-dimensionalization with reference exit conditions(p_o, u_o), the following equation would be obtained:

$$P_x\left[1 - 2/3\gamma\pi Kn_o^2 M_o^2\left(\frac{p_o}{p}\right)^2 U_y^2\right] = U_{yy} + O(\varepsilon) \quad (4)$$

Similarly, for the y momentum equation, the following expression could be derived:

$$P_y\left[1 + \frac{\gamma\pi}{3}Kn_o^2 M_o^2\left(\frac{p_o}{p}\right)^2 U_y^2\right] = \frac{4}{3}\sqrt{\gamma\pi/2}M_o Kn_o\left(\frac{p_o}{p}\right)U_y U_{yy} + O(\varepsilon) \quad (5)$$

Where Kn_o and M_o refer to the Knudsen and Mach numbers estimated at the outlet of the studied geometry respectively. These numbers are expressed as follows:

$$Kn_o = \frac{\mu_o}{\rho_o\sqrt{RT_o}H} \quad (6)$$

$$M_o = \frac{u_o}{\sqrt{\gamma RT_o}} \quad (7)$$

The $Kn_o^2 M_o^2 (p_o/p)^2$ term is relatively small for low Mach number flows in the early transition regime. In this case, for flow through a very long channel, the Burnett equations are reduced to:

$$P_x = U_{yy} \quad (8)$$

$$P_y = \frac{4}{3}\sqrt{\gamma\pi/2}M_o Kn_o\left(\frac{p_o}{p}\right)U_y U_{yy} \quad (9)$$

3. Slip boundary conditions

Non-slip boundary conditions are generally unrealistic for transition flows since the collisions near a wall are insufficient to equilibrate the flow field. Slip conditions should therefore be considered at such wall. Some researchers solved Burnett equations with first-order slip boundary conditions [9, 13], while others used the equations with second-order slip boundary conditions [11, 19]. The present work deviates from convention by imposing both types of boundary conditions on the calculations.

3.1. First-order slip boundary conditions

The first-order slip boundary conditions are written as follows [13]:

$$u_s - u_w = \frac{2-\sigma_u}{\sigma_u}\lambda\left.\frac{du}{dy}\right|_w \quad (10)$$

$$T_s - T_w = \frac{2-\sigma_T}{\sigma_T}\frac{2\gamma}{\Pr(\gamma+1)}\lambda\left.\frac{dT}{dy}\right|_w \quad (11)$$

where σ_u and σ_T are the tangential momentum and thermal accommodation coefficients, respectively, and subscripts s and w denote slip and wall values, respectively. In these conditions, the effects of thermal creep and quadratic variation with Kn are disregarded.

After non-dimensionalization with characteristic length L, Eqs. (10) and (11) take the forms

$$U_s^* - U_w^* = \frac{2-\sigma_u}{\sigma_u}Kn\left.\frac{\partial U^*}{\partial n^*}\right|_w \quad (12)$$

$$T_s^* - T_w^* = \frac{2-\sigma_T}{\sigma_T}\frac{2\gamma}{\gamma+1}\frac{Kn}{Pr}\left.\frac{\partial T^*}{\partial n^*}\right|_s \quad (13)$$

where $(\partial/\partial n^*)$ indicates gradients normal to the wall surface, and n^* = n/L.

3.2. Second-order slip boundary conditions

Some researchers believe that because Burnett equations are second-order solutions of the Boltzmann equation, the boundary conditions also require to be accurate at the second-order level in relation to Kn. Assuming that σ_u = 1 and $\sigma_T = 1$, the general second-order slip conditions have the following non-dimensional forms:

$$U_s^* - U_w^* = A_1 Kn \frac{\partial U_s^*}{\partial n^*} + A_2 Kn^2 \frac{\partial^2 U_s^*}{\partial n^{*2}} \quad (14)$$

$$T_s^* - T_w^* = \left(\frac{2\gamma}{\gamma+1}\right)\left(\frac{1}{Pr}\right)\left[Kn\left(\frac{\partial T^*}{\partial n^*}\right)_s + \frac{Kn^2}{2}\left(\frac{\partial^2 T^*}{\partial n^{*2}}\right)_s\right] \quad (15)$$

Where coefficients A_1 and A_2 are the slip coefficients. Different typical values of slip coefficients were expanded by researchers [21]. In the present study,the values in the Deissler model [22] are adopted, which indicates that A_1 = 1 and A_2 =–9/8. In Eq. (15), Pr and γ are the Prandtl number and the ratio of specific heat, respectively.

4. Solution procedure and results

On the basis of Eq. (8), velocity distribution can be modeled as a parabolic phenomenon in the transition regime, with a compatible slip condition as follows:

$$U^*(x,y) = f(\frac{dP}{dx}, \mu_o, H, \lambda)[-(y^*)^2 + ay^* + b] \quad (16)$$

Where $f(dp/dx, \mu_o, H, \lambda)$ reflects the functional dependence of velocity on pressure gradient, viscosity, channel height, and local mean free path.

The integration of the velocity distribution derived from Eq. (14) over the cross-section of the micro-Couette geometry leads to the mean velocity
as below:

$$\bar{U} = \frac{1}{2}\int_{-1}^{1} U^* dy^* = \int_0^1 U^* dy^* = f\left(\frac{dP}{dx}, \mu_o, h, \lambda\right)\left[-\frac{1}{3} + \frac{a}{2} + b\right] \quad (17)$$

The utilization of the first-order slip boundary conditions in Eq. (12) for the two upper and lower walls of the micro-Couette geometry renders the problem in the following form:

$$U^*|_{y^*=0} = U_s^* = Kn \left.\frac{\partial U^*}{\partial y^*}\right|_{y^*=0} \quad (18)$$

$$U^*|_{y^*=1} = U_w^* - Kn \left.\frac{\partial U^*}{\partial y^*}\right|_{y^*=1} \quad (19)$$

It was assumed that $U_w^* = 1$. Finally, solving Eq. (16) yields the following coefficients:

$$a = \frac{2(1+Kn)}{1+2K_n} \quad (20)$$

$$b = \frac{2Kn(1+Kn)}{1+2Kn} \quad (21)$$

Accordingly, the normalized velocity of flow in the micro-Couette geometry is reduced to:

$$U^{**}(y^*, Kn) = \frac{U^*}{\bar{U}} = \frac{-(y^*)^2 + \left(\frac{2+2Kn}{1+2Kn}\right)y^* + \frac{2Kn(1+Kn)}{1+2Kn}}{-\frac{1}{3} + \frac{2Kn^2+3Kn+1}{1+2Kn}} \quad (22)$$

Eq. (16) is solved again, this time with the second-order slip boundary conditions [22], and only coefficient b is modified as follows:

$$b = \frac{2Kn(1+Kn)}{1+2Kn} + (9/4)Kn^2 \quad (23)$$

The normalized velocity can also be changed into:

$$U^{**}(y^*, Kn) = \frac{U^*}{\bar{U}} = \frac{-(y^*)^2 + \left(\frac{2+2Kn}{1+2Kn}\right)y^* + \frac{2Kn(1+Kn)}{1+2Kn} + (9/4)Kn^2}{-\frac{1}{3} + [(9/4)Kn^2 + Kn + 1]} \quad (24)$$

Heat transfer is an important issue in Couette flow. Thus, Burnett equations are provided as the sum of corresponding Navier–Stokes and Burnett heat flux terms:

$$q_{ij} = (\mathrm{q_{ij}})^{\mathrm{N-S}} + (\mathrm{q_{ij}})^{\mathrm{B}} \quad (25)$$

For the Navier–Stokes equations, the terms are as follows:

$$(\mathrm{q_{ij}})^{\mathrm{N-S}} = -k\nabla T \quad (26)$$

Where k is the thermal conductivity of gas, and T denotes the temperature. For Burnett equations, q_{ij} for a fully developed incompressible flow in the micro-Couette geometry is the same as that in Navier–Stokes equations. A micro-Couette geometry with a lower adiabatic wall ($q_w|_{y^*=0} = 0$) and an upper wall with constant heat flux ($q_w|_{y^*=1} = q_h$) was considered. Flow was supposed to be hydrodynamically and thermally developed and incompressible, and fluid properties were assumed to be uniform. The energy equation is reduced into:

$$\frac{k}{H^2}\frac{\partial^2 T}{\partial y^{*2}} = \rho u c_p \frac{\partial T}{\partial x} \quad (27)$$

Disregarding viscous dissipation, the following parameter was introduced:

$$\theta^* = \frac{T - T_{wall}}{q_h H/k} \quad (28)$$

Where $q_h = \alpha(\bar{T} - T_{wall})$, and α is the convection heat transfer coefficient. Since the flow is thermally developed, the energy equation could be simplified as:

$$\frac{q_h}{H}\frac{\partial^2 \theta^*}{\partial y^{*2}} = \rho u c_p \frac{\partial \bar{T}}{\partial x} \quad (29)$$

The conservation of energy on a control volume of length dx and height H yields ($H\rho c_p \bar{u} d\bar{T} = -q_h dx$), thereby Eq. (29) would be reduced to:

$$\frac{d^2\theta^*}{dy^{*2}} = -\frac{U^*}{\bar{U}} \quad (30)$$

$$\frac{d^2\theta^*}{dy^{*2}} = \frac{(y^*)^2 - \left(\frac{2+2Kn}{1+2Kn}\right)y^* - \frac{2Kn(1+Kn)}{1+2Kn}}{-\frac{1}{3} + \frac{2Kn^2+3Kn+1}{1+2Kn}} \quad (31)$$

With thermal creep disregarded, the first-order slip boundary conditions are:

$$\left.\frac{d\theta^*}{dy^*}\right|_{y^*=0} = 0 \quad (32)$$

$$\theta^*|_{y^*=1} = -8\left(\frac{2-\sigma_T}{\sigma_T}\right)\left[\frac{\gamma}{\gamma+1}\right]\frac{Kn}{Pr}\left.\frac{d\theta^*}{dy^*}\right|_{y^*=1} \quad (33)$$

Using a monatomic ideal gas with $Pr = 2/3$ and $\gamma = 5/3$, it is possible to reduce the Eq. (33) to:

$$\theta^*|_{y^*=1} = -\frac{15}{8}Kn\left.\frac{d\theta^*}{dy^*}\right|_{y^*=1} \quad (34)$$

The integration of Eq. (31) with boundary conditions (32) and (34) yields:

$$\theta^*(y^*, Kn) = \frac{\left[\frac{1}{12}y^{*4} - \frac{1}{6}\left(\frac{2+2Kn}{1+2Kn}\right)y^{*3} - \frac{Kn(1+Kn)}{1+2Kn}y^{*2}\right]+m}{-\frac{1}{3}+\frac{2Kn^2+3Kn+1}{1+2Kn}} \quad (35)$$

The coefficient of m can be obtained as:

$$m = \left(-\frac{1}{12}\right)\left[1 + 30Kn - \frac{180Kn^3+282Kn^2+106Kn+4}{1+2Kn}\right] \quad (36)$$

Eq. (31) is also solved with the second-order slip boundary conditions. Thus,

$$\left.\frac{d\theta^*}{dy^*}\right|_{y^*=0} = 0 \quad (37)$$

$$\theta^*|_{y^*=1} = \left(\frac{15}{8}Kn\right)\left[-\left.\frac{d\theta^*}{dy^*}\right|_{y^*=1} + \left(\frac{Kn}{2}\right)\left.\frac{d^2\theta^*}{dy^{*2}}\right|_{y^*=1}\right] \quad (38)$$

In this case, the coefficient of m can be modified as follows:

$$m = \left(\frac{15}{16}Kn - \frac{15}{16}Kn^2 + \frac{1}{6}\right)\left(\frac{2+2Kn}{1+2Kn}\right)$$
$$+\left(\frac{15}{8}Kn - \frac{15}{16}Kn^2 + \frac{1}{2}\right)\left(\frac{2K_n(1+Kn)}{1+2Kn}\right)$$
$$+\left(\frac{15}{16}Kn^2 - \frac{5}{8}Kn - \frac{1}{12}\right) \quad (39)$$

5. Discussion

In micro-Couette geometry where the transition flow regime is subjected to a pressure gradient of zero, Burnett equations are reduced to:

$$U_{yy} = 0 \quad (40)$$

In order to validate the results, gas flow was considered as the flow between two infinitely long and wide parallel plates separated by a distance H. These plates move in opposite directions with equal velocity (U_O/2). The integration of Eq. (40) with the first-order slip boundary conditions therefore generates a linear velocity profile as:

$$U = \left(\frac{1/2}{Kn+1/2}\right)y^* \quad (41)$$

The values obtained from the equation above for Kn = 0.3, 0.5 show good agreement with those obtained by Singh *et al*. [12] via the DSMC method (Fig. 2). The small error at Kn = 0.5 is due to the accuracy of the method by which the Burnett equations were simplified.

Figs. 3 and 4 present the normalized velocity profile obtained from the Burnett equations with first- and second-order boundary conditions, respectively. The normalized velocity obtained on the basis of the first-order boundary conditions (Eq. (22)) approach and the normalized velocity derived with the second-order boundary conditions (Eq. (24)). The velocity profile flattens with increasing Knudsen number. Consequently, it could be concluded that with increasing the Knudsen number, the slip on the wall improves, and the effect of upper plate velocity would decrease.

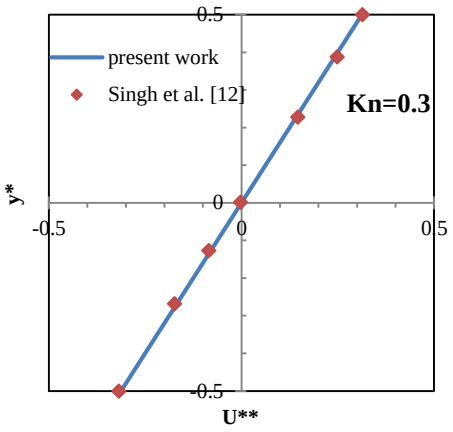

$(a)\ Kn = 0.3$

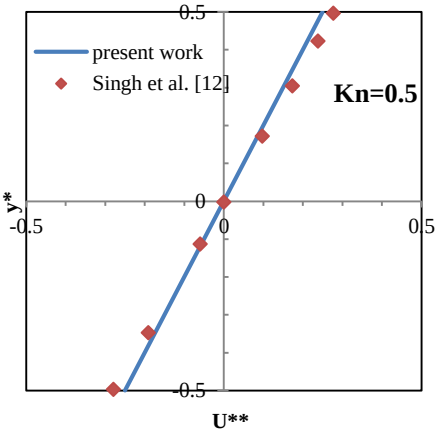

$(b)\ Kn = 0.5$

Figure 2. Comparison of non-dimensional velocity profiles in the present work and in Singh et al. [12] (via DSMC) for different Kn numbers.

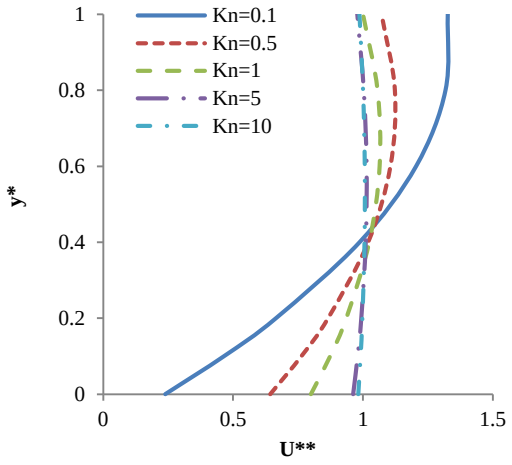

Figure 3. Variations in normalized velocity across the channel, derived using Burnett equations with first-order slip boundary conditions.

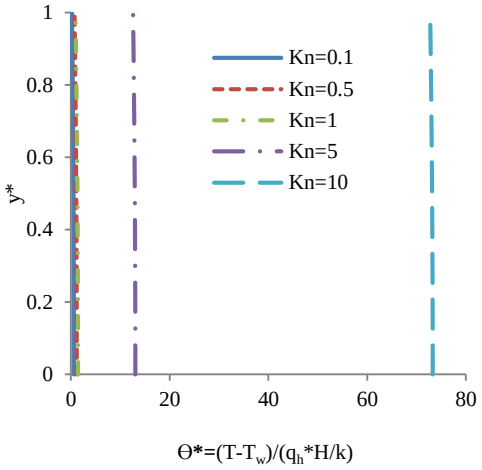

Figure 6. Non-dimensional temperature profile derived using Burnett equations with second-order slip boundary conditions.

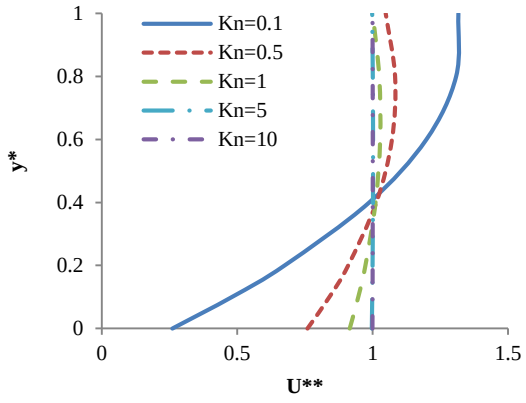

Figure 4. Variations in normalized velocity across the channel, derived using Burnett equations with second-order slip boundary conditions.

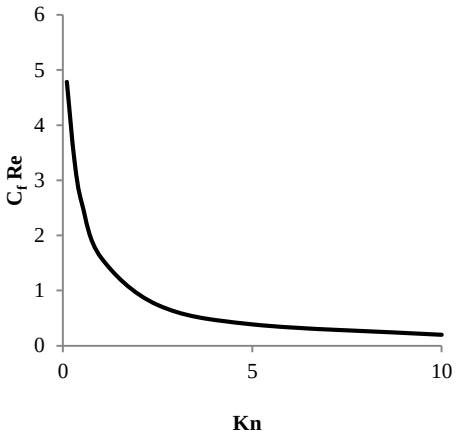

Figure 7. Variations in the product of the friction factor and Reynolds number with Knudsen number.

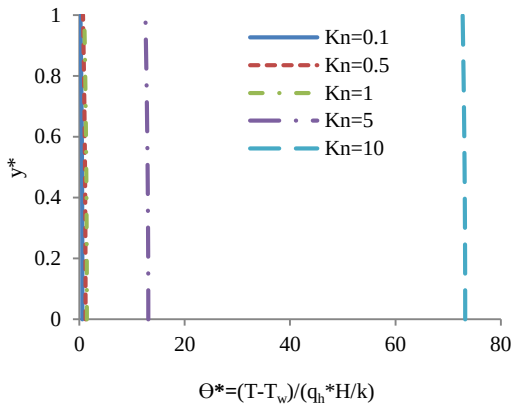

Figure 5. Non-dimensional temperature profile derived using Burnett equations with first-order slip boundary conditions.

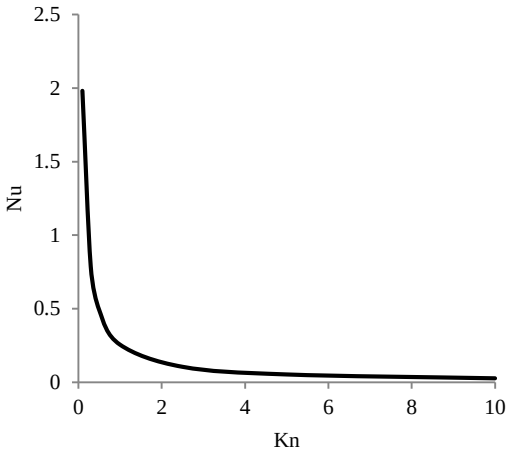

Figure 8. Variations in Nu with Kn.

Another integral parameter of interest to the engineering group is the skin friction coefficient (C_f). The Poiseuille number (Po) is explained as the product of the friction factor and Reynolds number as:

$$C_f = \frac{\tau_w}{\frac{1}{2}\rho\bar{U}^2} = \frac{\mu\frac{\partial U}{\partial y}\Big|_{y=0}}{\frac{1}{2}\rho\bar{U}^2} = \frac{\frac{\bar{U}}{h}\mu\frac{\partial U^*}{\partial y^*}\Big|_{y^*=0}}{\frac{1}{2}\rho\bar{U}^2} \quad (42)$$

$$C_f = \left(\frac{2\mu}{h\rho\bar{U}}\right)\frac{\partial U^*}{\partial y^*}\Big|_{y^*=0} = \left(\frac{2}{Re_h}\right)\frac{\partial U^*}{\partial y^*}\Big|_{y^*=0} \quad (43)$$

$$P_o = C_f Re = 2\frac{\partial U^*}{\partial y^*}\Big|_{y^*=0} = \frac{2\left(\frac{2+Kn}{1+2Kn}\right)}{-\frac{1}{3}+\frac{2Kn^2+3Kn+1}{1+2Kn}} \quad (44)$$

Fig. 7, which presents variations in the Poiseuille number with Knudsen number, reveals that the former decreases with an increase in the latter.

With Eq. (28), T and $\bar{T} = \int_0^1 (U^*/\bar{U})T\,dy^*$ are calculated, and the Nusselt number is obtained as:

$$Nu = \frac{2q_h H}{k(\bar{T}-T_w)} = \frac{2(T-T_w)}{\theta^*(\bar{T}-T_w)} \quad (45)$$

Fig. 8 demonstrates that Nu decreases with increase of the Kn. This behavior can be described on the basis of Fig. 4., which indicates that with increasing Knudsen number, θ^* rapidly increases, thereby reducing Nu (see Eq. (45)).

6. Conclusion

The present study was an attempt to the analytical solution of pressure- and shear-driven micro-Couette flow in terms of Burnett equations in the transition regime. The equations were simplified and solved for stress and heat flux terms by imposing first- and second-order slip boundary conditions on micro-Couette flow. In the absence of an axial pressure gradient, the velocity profile behaves linearly, which indicates a good agreement with the results available in the literature. By applying a pressure gradient in the direction of flow, the velocity profile behaved parabolically.

The normalized velocity obtained via the first-order slip boundary conditions is approximately similar to that derived through the second-order slip boundary conditions. However, the non-dimensional temperature profiles obtained using the conditions considerably differ at Kn>1. Additionally, the non-dimensional velocity and temperature profiles at a large Kn are flatter than those at a small Kn. This finding is due to the fact that an increasing Knudsen number elevates the slip on the wall and decreases the curvature of the profiles. Furthermore, the Poiseuille and Nusselt numbers rapidly decrease with increase of the Kn.

To sum up, the Burnett equations have been manifested to be an extremely good technique for solution of simple gas flows in microfluidic applications, especially for high values of the Kn number. As for a future work, Burnett equations could be utilized for more complex two-dimensional geometries and three-dimensional micro flow problems.

Nomenclature

C_f	friction factor
C_p	heat capacity
H	micro-Couette height
k	thermal conductivity
Kn	Knudsen number
L	micro-Couette length
M	Mach number
Nu	Nusselt number
Pr	Prandtl number
p	pressure
q	heat flux
R	specific gas constant
Re	Reynolds number
T	temperature
u	axial velocity
v	vertical velocity

Greek symbols

α	convection heat transfer coefficient
γ	ratio of specific heat
ε	ratio of channel height to length
λ	mean free path
μ	viscosity
ρ	density
σ_T	thermal accommodation coefficient
σ_u	tangential momentum accommodation coefficient
τ	shear stress

Superscripts and subscripts

i	inlet
o	outlet
s	slip
x,y	cross-sectional coordinates
w	wall
∗	non-dimensional parameters
**	normalized velocity
-	averaged quantities

References

[1] M. Shamshiri, M. Ashrafizaadeh, E. Shirani, "Investigation of flow and heat transfer characteristics of rarefied gaseous slip in nonplanar micro-Couette configuration," International Journal of Thermal Sciences, 54, 262-275, (2012).

[2] H. Shokouhmand, A.H. Meghdadi Isfahani, E. Shirani, "Friction and heat transfer coefficient

in micro and nano channels filled with porous media for wide range of Knudsen number," International Communications in Heat and Mass Transfer, 37, 890-894, (2010).

[3] M. Mirzaei, M. Dehghan, "Investigation of flow and heat transfer of nanofluid in microchannel with variable property approach," Heat and Mass Transfer, 49, 1803-1811, (2013).

[4] M. Dehghan, M. Daneshipour, M.S. Valipour, R. Rafee, S. Saedodin, "Enhancing heat transfer in microchannel heat sinks using converging flow passages," Energy Conversion and Management, 92, 244-250, (2015).

[5] M. Dehghan, M.S. Valipour, S. Saedodin,Y. Mahmoudi "Investigation of forced convection through entrance region of a porous-filled microchannel: An analytical study based on the scale analysis," Applied ThermalEngineering, 99, 446-454, (2016).

[6] Y. Demirel, "Thermo dynamic analysis of thermo mechanical coupling in Couette flow," International Journal of Heat and Mass Transfer, 43, 4205-4212, (2000).

[7] M. Budair, "Entropy analysis of unsteady flow on flat plate," international journal renewable energy research, 25, 519-524, (2001).

[8] L. S. Garcia-Colin, R. M. Velasco, F. J. Uribe, "Beyond the Navier-Stokes: Burnett hydrodynamics," Physics Reports, 465, 149–189, (2008).

[9] H. Xue, H. M. Ji, C. Shu, "Analysis of micro-Couette flow using the Burnett equations," International Journal of Heat and Mass Transfer, 44, 4139–4146, (2001).

[10] P. L. L. Walls, B. Abedian, "Bivelocity gas dynamics of micro-channel," International Journal of Engineering Science, 79, 21–29, (2014).

[11] N. Singh, N. Dongari, A. Agrawal, "Analytical solution of plan Poiseuille flow within Burnett hydrodynamics," Microfluid Nanofluid, 1224-1227, (2013).

[12] N. Singh, A. Gavasane, A. Agrawal, "Analytical solution of plane Couette flow in the transition regime and comparison with Direct Simulation Monte Carlo data," Computers & Fluids, 97, 177-187, (2014).

[13] D. A. Lockerby, J. M. Reese, "High resolution Burnett simulations of micro Couette flow and heat transfer," journal of computational physics, 188, 333–347, (2003).

[14] H. Xue, H. M. Ji, C. Shu, "Prediction of flow and heat transfer characteristics in micro Couette flow," Microscale Thermo physical Engineering, 7 (2), 51–68, (2003).

[15] W. A. Zahid, Y. Yin, K. Zhu, "Couette-Poiseuille flow of a gas in long micro channels," Microfluid Nanofluid, 3, 55-64, (2007).

[16] A. Beskok, G. E. Karniadakis, W. Trimmer, "Rarefaction and compressibility effects in gas microflows," ASME journal of fluids engineering, 118, 448–456, (1996).

[17] J. Jang, S.T. Wereley, "Pressure distributions of gaseous slip flow in straight and uniform rectangular microchannels," Microfluid Nanofluid, 1, 41–51, (2004).

[18] F. Bao, J. Lin, "Burnett simulation of gas flow and heat transfer in micro Poiseuille flow," International Journal of Heat and Mass Transfer, 51, 4139–4144, (2008).

[19] G. E. Karniadakis, A Beskok, N. Aluru, Microflows and Nanoflows: fundamentals and simulation, Springer, NewYork, 66-145, (2005).

[20] R. Schamberg, The Fundamental Differential Equations and the Boundary Conditions for High Speed Slip Flow and Their Application to Several Specific Problems, PhD thesis, California Institute of Technology (1947).

[21] S. Kandlikar, S.Garimella, D. Li, S. Colin, M. R. King, Heat Transfer and Fluid flow in Minichannels and Microchannels, Elsevier Science, (2005).

[22] R.G. Deissler, "An analysis of second order slip flow and temperature-jump boundary conditions for rarefied gases," Heat and Mass Transfer, 7, 681–694, (1964).